

Article

Synthesis and Biological Evaluation of Novel Synthetic Indolone Derivatives as Anti-Tumor Agents Targeting p53-MDM2 and p53-MDMX

Yali Wang ^{1,*}, Bo Ji ¹, Zhongshui Cheng ¹, Lianghui Zhang ¹, Yingying Cheng ¹, Yingying Li ¹, Jin Ren ¹, Wenbo Liu ¹ and Yuanyuan Ma ²

¹ School of Pharmacy and Life Sciences, Jiujiang University, Jiujiang 332000, China; xhawx233@163.com (B.J.); csz13479842156@163.com (Z.C.); jjbio@126.com (L.Z.); m15807983494@163.com (Y.C.); 19142049457@163.com (Y.L.); yanjiushengrj@126.com (J.R.); bowenliu2008@163.com (W.L.)

² Institute of Medicinal Biotechnology, Chinese Academy of Medical Science and Peking Union Medical College, Beijing 100050, China; mayuanyuancircle@163.com

* Correspondence: yaliwang@jju.edu.cn

Abstract: A series of novel indolone derivatives were synthesized and evaluated for their binding affinities toward MDM2 and MDMX. Some compounds showed potent MDM2 and moderate MDMX activities. Among them, compound A13 exhibited the most potent affinity toward MDM2 and MDMX, with a K_i of 0.031 and 7.24 μ M, respectively. A13 was also the most potent agent against HCT116, MCF7, and A549, with IC_{50} values of 6.17, 11.21, and 12.49 μ M, respectively. Western blot analysis confirmed that A13 upregulated the expression of MDM2, MDMX, and p53 by Western blot analysis. These results indicate that A13 is a potent dual p53-MDM2 and p53-MDMX inhibitor and deserves further investigation.



Citation: Wang, Y.; Ji, B.; Cheng, Z.; Zhang, L.; Cheng, Y.; Li, Y.; Ren, J.; Liu, W.; Ma, Y. Synthesis and Biological Evaluation of Novel Synthetic Indolone Derivatives as Anti-Tumor Agents Targeting p53-MDM2 and p53-MDMX. *Molecules* **2022**, *27*, 3721. <https://doi.org/10.3390/molecules27123721>

Academic Editor: Qiao-Hong Chen

Received: 16 May 2022

Accepted: 8 June 2022

Published: 9 June 2022

Publisher's Note: MDPI stays neutral with regard to jurisdictional claims in published maps and institutional affiliations.



Copyright: © 2022 by the authors. Licensee MDPI, Basel, Switzerland. This article is an open access article distributed under the terms and conditions of the Creative Commons Attribution (CC BY) license (<https://creativecommons.org/licenses/by/4.0/>).

Keywords: p53-MDM2; p53-MDMX; indolone derivatives; anti-tumor

1. Introduction

Tumor suppressor p53 plays a crucial role in the regulation of DNA repair, cell cycle, apoptosis, and differentiation [1,2]. It is inactivated in the majority of human cancers, resulting from mutations or the overexpression of its negative regulators, murine double minute 2 (MDM2) and/or murine double minute X (MDMX) [3]. Approximately 50% of human cancers have a p53 gene mutation and may be combated using gene therapy. For the remaining cancer types, the function of p53 can be reactivated by disrupting the interaction with MDM2 and MDMX proteins using small-molecule inhibitors [4]. Therefore, the interfaces of p53-MDM2 and p53-MDMX have emerged as important targets for the development of novel chemotherapeutic agents.

To date, over 20 chemotypes have been reported as p53-MDM2 inhibitors including nutlins [5], spiro-oxindole [6], benzodiazepinedione [7], isoquinolin-1-one [8], chromenotriazolopyrimidines [9], imidazolyl indole [10], piperidine [11], chalcone [12], diketopiperazines [13], morpholinone [14], pyrrolin-2-one [15], and many others. Several p53-MDM2 inhibitors such as RG7112 [16], RG7388 [17], SAR405838 [18], AMG-232 [19], HDM201 [20], and APG-115 [21] (Figure 1) have progressed into clinical trials. However, p53-MDM2 inhibitors are inadequate when MDMX is also expressed at a high level in some cancer cells. A few p53-MDMX inhibitors have also been reported such as SJ-172550 [22], NSC207895 [23], and NSC146109 [24].

Studies have verified that dual MDM2/MDMX inhibitors can activate p53 better than selective inhibitors that only target MDM2 or MDMX [25]. Currently, some progress has been made in designing dual inhibitors of MDM2 and MDMX [26–30]. ALRN-6924 (Figure 1), a dual inhibitor of MDM2 and MDMX, has gone into a phase I clinical trial

(NCT04022876) in patients with solid tumors [31]. However, there are many challenges that need to be overcome before use in clinical practice and novel inhibitors need to be developed.

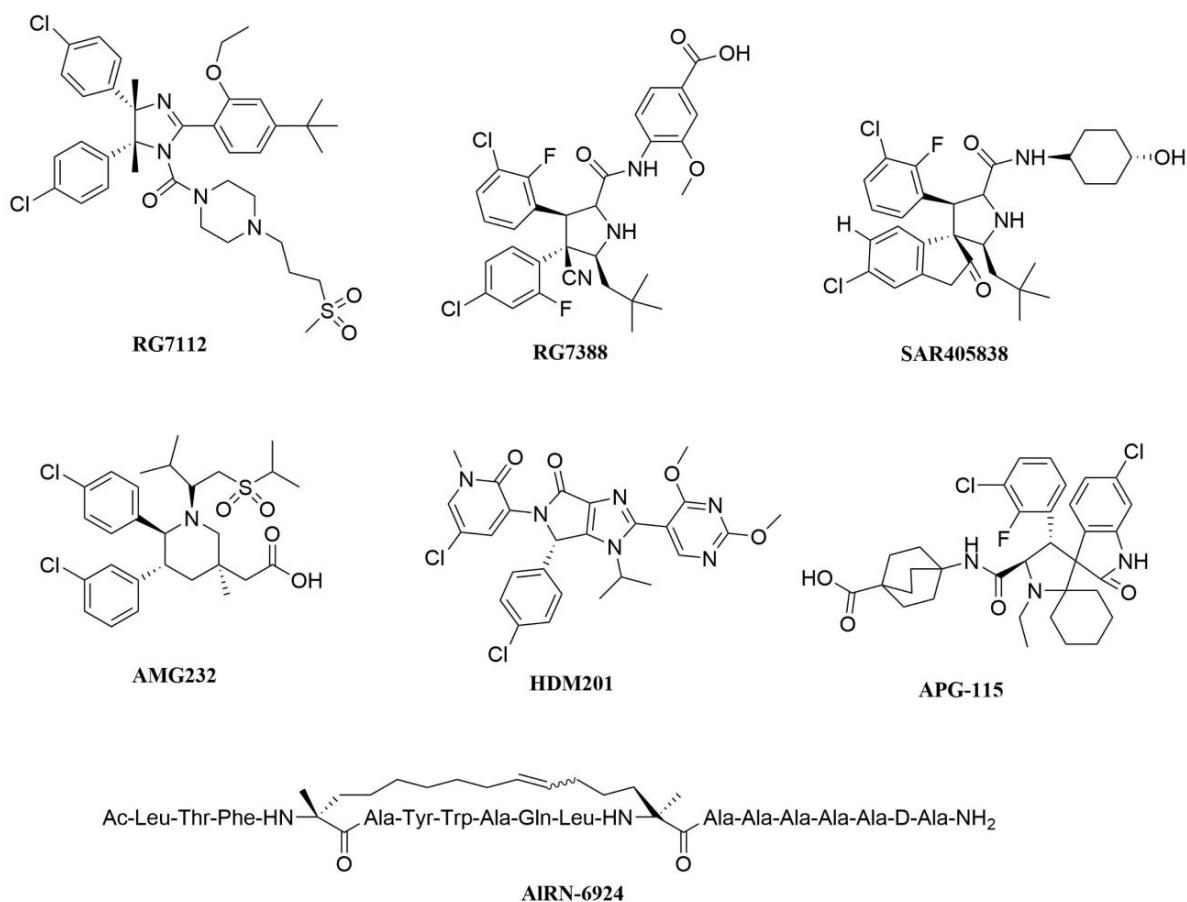


Figure 1. Representative structures of the p53-MDM2 and p53-MDM2/MDMX inhibitors entering clinical studies.

Indole, as a heterocyclic molecule, is a significant source of the pharmacologically active compound. Due to its chemical reactivity, indole could be modified to obtain many indole derivatives, exhibiting a variety of bioactivities. Especially as anti-cancer agents, indoles are effective against a variety of cancers including acute myeloid leukemia [32,33], lung cancer [34], cervical cancer [35], colon cancer, breast cancer [36], and others. The targets of indoles as anti-cancer agents were also reported such as the Mcl-1, Pim, HDAC, SIRT, tubulin [32,37], RAF-MEK-ERK, and PI3K-PDK1-AKT pathways [34], and so on. Some indole derivatives have even been identified as very promising candidates for phototherapy application against highly aggressive and resistant cancers [38].

As shown in Figure 2, some indole derivatives, which are reported as anti-cancer agents targeting MDM2 and MDMX (1b, RO-2443) [36,39], have been modified to improve the activities and explore new mechanisms. In the present study, novel indolone compounds were identified and the derivatives were synthesized and evaluated for their affinities toward MDM2 and MDMX. The most active compounds were tested for their *in vitro* anti-tumor activity against the MCF7, HCT116, and A549 cell lines to verify their antiproliferative activity.

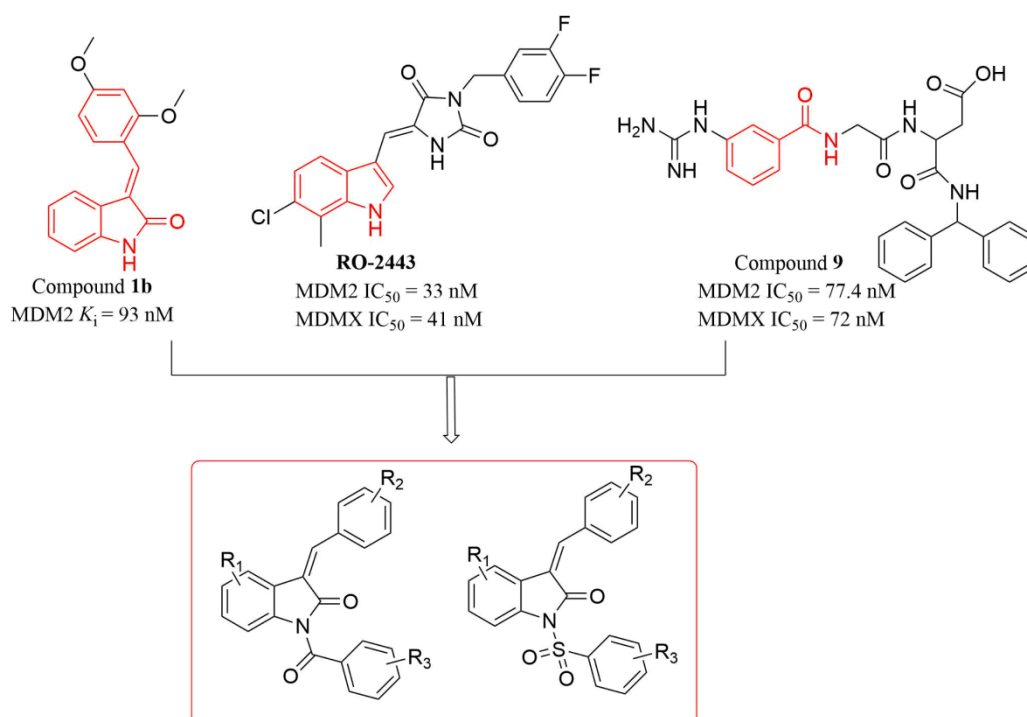
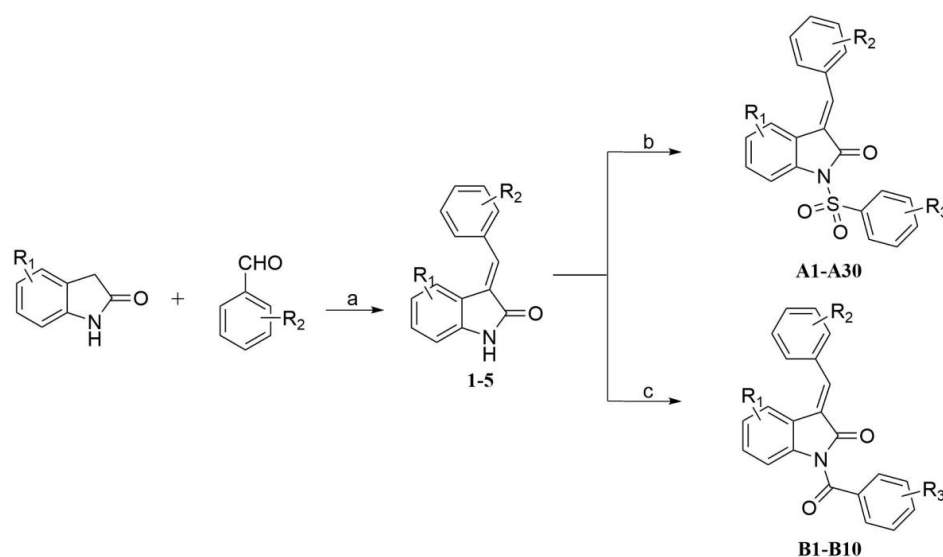


Figure 2. The design strategy of the target compounds.

2. Results and Discussion

2.1. Chemistry

Compounds **A1–A30** and **B1–B10** were synthesized according to Scheme 1. A condensation reaction was carried out to obtain intermediate compounds **1–5** with the commercially available substituted oxindole and benzaldehyde materials. Next, compounds **1–5** were sulfonylated or acylated to obtain **A1–A30** and **B1–B10**, with corresponding benzene sulfonyl chloride or benzoyl chloride in the presence of sodium hydroxide in tetrahydrofuran. In total, 40 derivatives were synthesized and the compound structures are listed in Table 1. The ^1H NMR spectrum, ^{13}C NMR spectrum, and mass spectrum of compounds **1–5**, **A1–A30**, and **B1–B10** were listed in the Supplementary Materials.



Scheme 1. The synthetic route for target compounds **A1–A30** and **B1–B10**. Reagents and conditions: (a) EtOH, NaOH, 60 °C, 4 h; (b) Substituted benzenesulfonyl chloride, NaOH, THF, 0–5 °C, 1–1.5 h; (c) Substituted benzoyl chloride, NaOH, THF, 0–5 °C, 1–1.5 h.

Table 1. The MDM2 and MDMX binding affinity of the synthesized compounds.

Compd.	R ₁	R ₂	R ₃	K _i (μM) ± SD	
				MDM2	MDMX
A1	H	2-Cl	H	4.39 ± 0.82	>50
A2	H	2-Cl	2-CH ₃	7.23 ± 1.03	>50
A3	H	2-Cl	3-CH ₃	5.58 ± 0.99	>50
A4	H	2-Cl	4-CH ₃	10.16 ± 1.45	>50
A5	H	2-Cl	2-Cl	3.43 ± 0.57	42.1 ± 6.35
A6	H	2-Cl	3-Cl	0.92 ± 0.11	17.43 ± 2.78
A7	H	2-Cl	4-Cl	1.53 ± 0.19	20.38 ± 2.62
A8	H	3-Cl	H	1.47 ± 0.15	10.33 ± 1.45
A9	H	3-Cl	2-CH ₃	6.95 ± 0.97	>50
A10	H	3-Cl	3-CH ₃	5.36 ± 1.06	>50
A11	H	3-Cl	4-CH ₃	5.19 ± 1.25	>50
A12	H	3-Cl	2-Cl	0.19 ± 0.05	20.83 ± 2.01
A13	H	3-Cl	3-Cl	0.031 ± 0.007	7.24 ± 0.78
A14	H	3-Cl	4-Cl	0.082 ± 0.021	18.19 ± 1.39
A15	H	3-Cl	2-Br	0.34 ± 0.12	24.37 ± 2.57
A16	H	3-Cl	3-Br	0.079 ± 0.005	16.21 ± 1.94
A17	H	3-Cl	4-Br	0.49 ± 0.15	43.18 ± 4.95
A18	H	3-Cl	2-F	0.17 ± 0.03	17.69 ± 2.16
A19	H	3-Cl	3-F	0.076 ± 0.005	16.89 ± 1.74
A20	H	3-Cl	4-F	0.23 ± 0.02	29.16 ± 3.51
A21	H	3-Cl	3-CF ₃	0.092 ± 0.007	19.26 ± 2.69
A22	H	3-Cl	3-NO ₂	1.39 ± 0.21	13.57 ± 1.47
A23	H	3-Cl	4-OCH ₃	3.77 ± 0.45	42.17 ± 4.73
A24	H	4-Cl	2-CH ₃	3.17 ± 0.37	34.69 ± 4.02
A25	H	4-Cl	3-CH ₃	4.93 ± 0.47	>50
A26	H	4-Cl	4-CH ₃	4.68 ± 0.39	>50
A27	H	4-Cl	3-Cl	0.31 ± 0.03	17.26 ± 1.91
A28	H	4-Cl	H	2.18 ± 0.29	37.43 ± 3.57
A29	5-Cl	3-Cl	3-Cl	0.28 ± 0.04	32.24 ± 3.24
A30	6-Cl	3-Cl	3-Cl	1.39 ± 0.15	28.96 ± 2.18
B1	H	2-Cl	2-Cl	10.17 ± 2.01	>50
B2	H	2-Cl	3-Cl	8.43 ± 1.58	>50
B3	H	2-Cl	4-Cl	7.86 ± 1.34	>50
B4	H	2-Cl	2-CH ₃	16.35 ± 2.77	>50
B5	H	2-Cl	3-CH ₃	20.19 ± 3.05	>50
B6	H	2-Cl	4-CH ₃	22.37 ± 3.64	>50
B7	H	3-Cl	2-Cl	14.87 ± 2.37	>50
B8	H	3-Cl	3-Cl	8.63 ± 1.55	>50
B9	H	3-Cl	4-Cl	15.92 ± 1.96	>50
B10	H	4-Cl	3-Cl	12.49 ± 1.04	>50
Nutlin-3a	-	-	-	0.15 ± 0.02	>50

2.2. In Vitro Enzymatic Assays and Structure–Activity Relationships

The MDM2 and MDMX binding evaluation for the target compounds was carried out using the fluorescence polarization assay. The bioactivity data are summarized in Table 1, where nutlin-3a was used as the positive control. The assay was validated by nutlin-3a with a K_i value of 0.15 μM, which is comparable to the previously reported value [40]. In general, all of the synthesized compounds (A1–A30 and B1–B10) showed a moderate to high binding affinity to MDM2. Most of the A1–A30 compounds showed a moderate binding affinity to MDMX. None of the B1–B10 compounds showed MDMX activities.

Compound A1 ($R_1 = H$, $R_2 = 2-Cl$, $R_3 = H$) demonstrated a moderate binding affinity to MDM2 ($K_i = 4.39$ μM). The introduction of methyl on sulfonyl moiety (A2–A4, $R_3 = 2-CH_3$, $3-CH_3$, $4-CH_3$) led to a lower potency compared to that of A1. However, compounds A5–A7 with a chlorine group ($R_3 = 2-Cl$, $3-Cl$, $4-Cl$) showed greater activity than A1. Compared to A1, when the R_2 2-Cl group was replaced with 3-Cl, A8 exhibited a potency

that was three-fold higher. Surprisingly, the introduction of a chlorine group to R_3 of **A8** (**A12–A14**, $R_3 = 2\text{-Cl}$, 3-Cl , 4-Cl) contributed to an obvious enhancement in activity, with a K_i of 0.19, 0.031 and 0.082 μM , respectively. **A13** and **A14** especially showed a greater potency than nutlin-3a. However, the results were not satisfactory when the methyl group was introduced to the same position (**A9–A11**). This phenomenon indicates that an electron-withdrawing group might be needed to increase the enzyme affinity. Other electron-withdrawing groups were introduced in subsequent experiments including the bromine, fluorine, trifluoromethyl, and nitro groups. Compounds **A16**, **A19**, and **A21** with the 3-substituted electron-withdrawing R_3 group exhibited more potency than the compound with 2-substituted or 4-substituted group (**A15**, **A17**, **A18**, and **A20**). **A16**, **A19**, and **A21** exhibited an even higher potency than nutlin-3a. Compared to **A1** and **A8**, when the 2-Cl or 3-Cl group of R_2 was replaced with 4-Cl, **A28** exhibited a lower activity than **A8**, but greater than **A1**. Next, structure modification was carried out at the position of R_3 (**A23–A27**) with K_i values of $>1 \mu\text{M}$. **A29** and **A30** showed a lower activity than **A13** with the introduction of the chlorine atom to R_1 (5-Cl and 6-Cl). Among the **B1–B10** compounds with benzoyl groups, **B3** showed the most potency with a K_i of 7.86 μM , which was lower than the A series with benzene sulfonyl groups.

Potency analysis of the compounds toward MDMX was carried out in the following assays. **A13** was the most potent MDMX binder with a K_i of 7.24 μM . The K_i values of some compounds (**A5–A8**, **A12–A24**, and **A27–A30**) ranged from 10.33 to 43.18 μM , while the rest of the compound values were $>50 \mu\text{M}$. Despite the significant homology of MDM2 and MDMX, the affinities of the same compound were notably different.

In general, the results listed in Table 1 showed that the activity of compounds **A1–A30** was better than that of compounds **B1–B10**, demonstrating that the introduction of the benzene sulfonyl chloride group led to a greater potency than the benzoyl chloride group. Compound **A13** showed the most potent affinity toward MDM2 and MDMX, with a K_i of 0.031 and 7.24 μM , respectively.

2.3. In Vitro Anti-Tumor Activities

The anti-tumor activities of the most active compounds with $K_i < 1 \mu\text{M}$ toward MDM2 in the fluorescence polarization assay were evaluated against the MCF7, HCT116, and A549 cell lines in vitro using the standard MTT assay, with nutlin-3a as a positive control.

As illustrated in Table 2, all compounds showed anti-tumor activities. Except for **A15**, **A16**, and **A17**, all of the other tested compounds showed a greater potency against HCT116 than nutlin-3a. **A13**, in particular, exhibited satisfactory potency, with an IC_{50} of 6.17 μM , which was about three-fold greater compared to that of nutlin-3a. The IC_{50} values of the tested compounds against MCF7 ranged from 11.21 to 37.70 μM . Twelve compounds showed a greater activity than nutlin-3a. **A13** and **A21** were the most potent agents against A549, with IC_{50} values of 12.49 and 13.48 μM , respectively, which were superior to the positive control.

In general, all of the tested compounds showed a better potency against HCT116 than MCF7 and A549. **A13** was the most potent compound against HCT116, MCF7, and A549, with IC_{50} values of 6.17, 11.21, and 12.49 μM , respectively. Surprisingly, **A13** exhibited the best enzymatic affinities as well as anti-tumor activities. Further research on **A13** was carried out in the following experiment.

2.4. Western Blotting Analyses

The dual inhibition of the p53-MDM2 and p53-MDMX interactions is expected to activate p53, increasing its level in the cells with wild-type p53. In addition, p53 activation can also result in an increase in the levels of the MDM2 and MDMX proteins. To verify these predictions, Western blotting was used to assess the effects of compound **A13** in the HCT 116 cells. The cells were treated with compound **A13** for 48 h. Subsequently, the cells were lysed and protein extracts were analyzed for the levels of p53, MDM2, and MDMX. As shown in Figure 3, compound **A13** caused a dose-dependent increase in the level of p53

proteins in HCT116 cells, indicating a good activation of p53. Expression of MDM2 and MDMX as well as the p53 downstream gene was also induced in a dose-dependent manner, which is consistent with the prediction. According to these results, it can be concluded that compound **A13** might exhibit anti-cancer activity through interrupting the p53-MDM2 and p53-MDMX interactions.

Table 2. The anti-tumor activities of several compounds against the HCT116, MCF7, and 143B cell lines in vitro.

Compd.	IC ₅₀ (μM)		
	HCT116	MCF7	A549
A6	10.72 ± 1.47	25.47 ± 3.61	18.72 ± 2.49
A12	15.36 ± 4.61	24.72 ± 2.53	17.83 ± 2.19
A13	6.17 ± 0.93	11.21 ± 1.95	12.49 ± 2.01
A14	15.18 ± 3.14	20.19 ± 2.86	20.33 ± 2.49
A15	23.79 ± 2.69	31.08 ± 3.55	29.12 ± 3.31
A16	21.73 ± 2.59	26.49 ± 3.40	25.44 ± 3.62
A17	25.47 ± 3.26	37.70 ± 3.65	34.17 ± 3.39
A18	17.88 ± 2.11	24.74 ± 3.63	22.58 ± 2.93
A19	10.15 ± 1.37	21.03 ± 2.58	16.27 ± 1.82
A20	16.32 ± 2.73	27.18 ± 2.83	22.19 ± 2.13
A21	8.91 ± 1.35	15.69 ± 2.04	13.48 ± 2.73
A27	17.49 ± 1.53	27.62 ± 3.81	20.36 ± 1.98
A29	16.96 ± 2.37	27.43 ± 3.37	26.35 ± 4.05
Nutlin-3a	18.13 ± 2.17	32.18 ± 1.49	21.72 ± 2.04

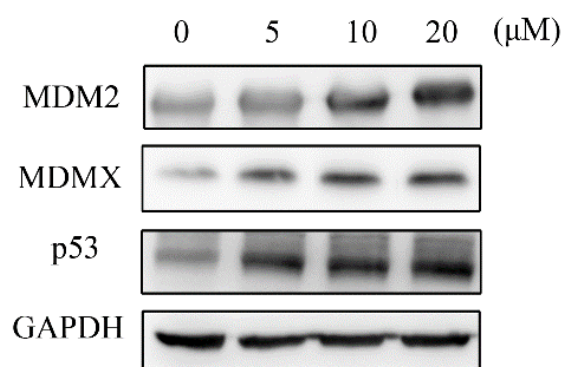


Figure 3. The Western blot analysis showing the expression of MDM2, MDMX, and p53 in the HCT116 cells treated with compound **A13**. GAPDH was included as a loading control.

2.5. Molecular Docking Analyses

Molecular docking was carried out and analyzed in order to observe the binding modes of compound **A13** in the active site of MDM2 and MDMX. The binding mode of compound **A13** in the MDM2 active site is shown in Figure 4A. The phenyl ring connected with the sulfonyl formed a non-classical H-bond with Tyr67, resulting in a hydrophobic interaction with Val93. The chlorine atom had σ - π and σ - σ hydrophobic interactions with His73 and Val93, respectively. The benzimidazole group formed a σ - π hydrophobic interaction with Val93 and σ - σ hydrophobic interactions with Val93 and Ile99. The phenyl connected with a double bond formed a σ - π hydrophobic interaction with His96, and the chlorine atom made σ - π , σ - σ , and σ - π hydrophobic interactions with His96, Ile99, and Tyr100, respectively. The binding mode of compound **A13** in the MDMX active site is shown in Figure 4B. The chlorobenzene group connected with sulfonyl formed σ - π and σ - σ hydrophobic interactions with Val92 and Met53. The benzimidazole group made σ - π hydrophobic interactions with Val92 and Ile60. The chlorobenzene connected with a double bond made σ - σ and σ - π hydrophobic interactions with Met61 and Tyr66, respectively. The

predicted K_i values of compound **A13** binding to MDM2 and MDMX were 0.018 and 5.18 μM , consistent with the test values.

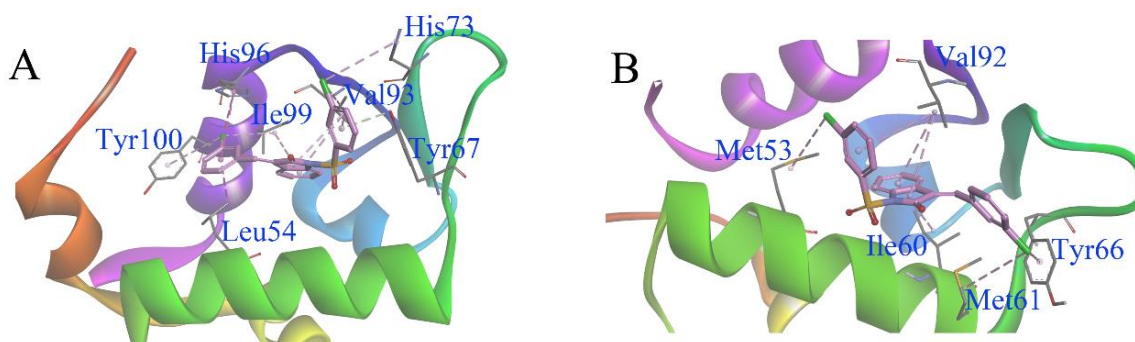


Figure 4. (A) The binding mode of compound **A13** in the active site of MDM2. (B) The binding mode of compound **A13** in the active site of MDMX. Compound **A13** is represented as stick diagrams with carbon atoms shown in pink.

From the docking results exhibited in Figure 4, the interactions between compound **A13** and MDM2 were obviously stronger than those of **A13** and MDMX, which might explain the different enzymatic activities of **A13** targeting MDM2 and MDMX.

3. Experimental Section

3.1. General Procedures

The mass spectra were acquired using an Agilent 6210 ESI/TOF or ThermoFisher Q Exactive mass spectrometer. ^1H and ^{13}C NMR spectra were recorded on a Bruker BioSpin GmbH spectrometer at 400 or 600 MHz. Column chromatography was performed on silica gel (200–300 mesh) from Qingdao Ocean Chemical. Unless specified, all reagents were obtained from commercially available sources.

3.2. General Procedure for Preparation of Intermediates (1–5)

A mixture of indolone (7.51 mmol), 2-chlorobenzaldehyde (7.51 mmol), and sodium hydroxide (7.51 mmol) in ethanol (30 mL) was stirred at 60 $^{\circ}\text{C}$ for 4 h. Then, the reaction mixture was allowed to cool to room temperature and added to the ice water. The precipitate was collected by filtration and purified using recrystallization with methanol to obtain the intermediates 1–5.

(Z)-3-(2-chlorobenzylidene)indolin-2-one (**1**): Yellow solid; yield: 85.2%; mp: 148.7–150.3 $^{\circ}\text{C}$; ^1H NMR (400 MHz, $\text{DMSO-}d_6$): δ 7.77–7.74 (m, 1H), 7.63 (dd, $J = 7.8, 1.9$ Hz, 1H), 7.57 (s, 1H), 7.52–7.47 (m, 2H), 7.22 (td, $J = 7.7, 1.0$ Hz, 1H), 7.12 (d, $J = 7.6$ Hz, 1H), 6.86 (d, $J = 7.7$ Hz, 1H), 6.79 (td, $J = 7.6, 0.9$ Hz, 1H); ^{13}C NMR (101 MHz, $\text{DMSO-}d_6$): δ 167.90, 143.06, 132.66, 131.19, 131.03, 130.42, 130.01, 129.61, 129.38, 127.21, 122.34, 121.02, 120.31, 110.07; MS calcd for $\text{C}_{15}\text{H}_{11}\text{ClNO}$ ($\text{M}+\text{H}$) $^+$ 256.05, found 256.05.

(Z)-3-(3-chlorobenzylidene)indolin-2-one (**2**): Yellow solid; yield: 79.3%; mp: 145.3–146.5 $^{\circ}\text{C}$; ^1H NMR (400 MHz, $\text{DMSO-}d_6$): δ 10.64 (s, 1H), 7.78–7.64 (m, 2H), 7.57–7.47 (m, 2H), 7.38 (d, $J = 7.5$ Hz, 1H), 7.24–6.96 (m, 2H), 6.87–6.80 (m, 2H). ^{13}C NMR (101 MHz, $\text{DMSO-}d_6$): δ 165.82, 144.72, 141.08, 138.51, 138.03, 131.95, 131.62, 130.37, 128.75, 127.14, 126.47, 124.24, 122.48, 114.21, 110.57; HRMS calcd for $\text{C}_{15}\text{H}_{11}\text{ClNO}$ ($\text{M}+\text{H}$) $^+$ 256.0529, found 256.0531.

(Z)-3-(4-chlorobenzylidene)indolin-2-one (**3**): Yellow solid; yield: 80.5%; mp: 144.6–145.7 $^{\circ}\text{C}$; ^1H NMR (400 MHz, $\text{DMSO-}d_6$): δ 10.64 (s, 1H), 7.72 (d, $J = 8.4$ Hz, 2H), 7.57 (d, $J = 8.2$ Hz, 3H), 7.47 (d, $J = 7.6$ Hz, 1H), 7.23 (t, $J = 7.6$ Hz, 1H), 6.88–6.83 (m, 2H); ^{13}C NMR (101 MHz, $\text{DMSO-}d_6$): δ 168.35, 142.95, 134.21, 134.01, 133.23, 131.02, 130.29, 128.75, 128.07, 122.36, 121.13, 120.53, 110.11; HRMS calcd for $\text{C}_{15}\text{H}_{11}\text{ClNO}$ ($\text{M}+\text{H}$) $^+$ 256.0529, found 256.0520.

(Z)-5-chloro-3-(4-chlorobenzylidene)indolin-2-one (**4**): Yellow solid; yield: 69.3%; mp: 192.9–193.8 $^{\circ}\text{C}$; ^1H NMR (400 MHz, $\text{DMSO-}d_6$): δ 8.65 (s, 1H), 8.17 (d, $J = 6.6$ Hz, 1H), 7.92

(s, 1H), 7.67–7.65 (m, 1H), 7.57 (d, $J = 5.0$ Hz, 1H), 7.51 (d, $J = 6.7$ Hz, 1H), 6.89 (d, $J = 9.0$ Hz, 1H), 6.83 (d, $J = 8.2$ Hz, 1H); ^{13}C NMR (101 MHz, DMSO- d_6): δ 166.69, 141.87, 139.61, 136.74, 135.58, 133.50, 130.93, 130.07, 129.94, 128.79, 127.57, 125.47, 121.83, 120.12, 110.85; HRMS calcd for $\text{C}_{15}\text{H}_{10}\text{Cl}_2\text{NO}$ ($\text{M}+\text{H}$) $^+$ 290.0139, found 290.0139.

(Z)-6-chloro-3-(4-chlorobenzylidene)indolin-2-one (**5**): Yellow solid; yield: 65.1%; mp: 195.6–197.1 °C; ^1H NMR (400 MHz, DMSO- d_6): δ 7.84–7.71 (m, 1H), 7.67–7.63 (m, 2H), 7.55–7.49 (m, 2H), 7.37 (d, $J = 8.2$ Hz, 1H), 6.91 (dd, $J = 10.2, 2.0$ Hz, 1H), 6.89–6.84 (m, 1H); ^{13}C NMR (101 MHz, DMSO- d_6): δ 168.26, 144.46, 136.38, 134.80, 133.51, 130.69, 129.50, 128.89, 127.60, 123.60, 121.01, 120.99, 119.47, 110.20, 109.45; HRMS calcd for $\text{C}_{15}\text{H}_{10}\text{Cl}_2\text{NO}$ ($\text{M}+\text{H}$) $^+$ 290.0139, found 290.0140.

3.3. General Procedure for Preparation of Target Compounds (A1–A30)

Sodium hydroxide (1.96 mmol) and corresponding benzene sulfonyl chloride (3 mmol) were added to a stirred solution of appropriate intermediates **1–5** (1.96 mmol) in 10 mL of anhydrous THF at 0 °C. The reaction mixture was stirred for 2 h. The organic solvent of the mixture was removed in vacuo and the residue was purified using column chromatography with petroleum ether/ethyl acetate (40:1–20:1) to obtain **A1–A30**.

(E)-3-(2-chlorobenzylidene)-1-(phenylsulfonyl)indolin-2-one (**A1**): solid; yield: 46.9%; mp: 138.2–139.9 °C; ^1H NMR (600 MHz, DMSO- d_6): δ 8.11 (d, $J = 7.6$ Hz, 2H), 7.92 (d, $J = 8.3$ Hz, 1H), 7.82 (t, $J = 7.5$ Hz, 1H), 7.75–7.70 (m, 4H), 7.66 (d, $J = 7.7$ Hz, 1H), 7.55 (t, $J = 7.2$ Hz, 1H), 7.47 (m, 2H), 7.23 (d, $J = 7.7$ Hz, 1H), 7.10 (t, $J = 7.7$ Hz, 1H); ^{13}C NMR (151 MHz, DMSO- d_6): δ 165.12, 138.61, 137.49, 135.39, 135.28, 132.89, 132.09, 132.03, 131.35, 130.23, 130.01, 129.93, 127.65, 127.45, 127.31, 126.09, 124.88, 122.86, 120.76, 113.50; HRMS calcd for $\text{C}_{21}\text{H}_{14}\text{ClNNaO}_3\text{S}$ ($\text{M}+\text{Na}$) $^+$ 418.0281, found 418.0263.

(E)-3-(2-chlorobenzylidene)-1-(o-tolylsulfonyl)indolin-2-one (**A2**): Yellow solid; yield: 59.3%; mp: 139.9–141.3 °C; ^1H NMR (600 MHz, DMSO- d_6): δ 8.08–7.99 (m, 1H), 7.89 (d, $J = 8.4$ Hz, 1H), 7.79 (d, $J = 7.1$ Hz, 1H), 7.76–7.73 (m, 1H), 7.71 (s, 1H), 7.69–7.66 (m, 1H), 7.57–7.56 (m, 2H), 7.52–7.48 (m, 3H), 7.26 (dd, $J = 7.5$ Hz, 1H), 7.12 (q, $J = 7.7, 7.5, 6.8$ Hz, 1H), 2.52 (s, 3H); ^{13}C NMR (151 MHz, DMSO- d_6): δ 139.69, 135.89, 135.35, 133.41, 133.29, 132.52, 132.47, 131.68, 131.17, 130.75, 130.70, 130.44, 128.08, 127.92, 127.23, 126.39, 125.15, 123.40, 114.06, 113.91; HRMS calcd for $\text{C}_{22}\text{H}_{16}\text{ClNNaO}_3\text{S}$ ($\text{M}+\text{Na}$) $^+$ 432.0437, found 432.0417.

(E)-3-(2-chlorobenzylidene)-1-(m-tolylsulfonyl)indolin-2-one (**A3**): Yellow solid; yield: 49.1%; mp: 140.2–141.9 °C; ^1H NMR (600 MHz, DMSO- d_6): δ 7.89 (t, $J = 3.9$ Hz, 2H), 7.73–7.71 (m, 2H), 7.64–7.61 (m, 2H), 7.59–7.52 (m, 3H), 7.48–7.44 (m, 2H), 7.20 (d, $J = 7.7$ Hz, 1H), 7.08 (t, $J = 7.7$ Hz, 1H), 2.40 (s, 3H); ^{13}C NMR (151 MHz, DMSO- d_6): δ 165.50, 140.29, 139.03, 137.85, 136.36, 135.79, 133.28, 132.48, 132.45, 131.78, 130.61, 130.42, 130.18, 128.07, 127.80, 126.53, 125.26, 125.07, 123.24, 121.10, 112.93, 21.24; HRMS calcd for $\text{C}_{22}\text{H}_{16}\text{ClNNaO}_3\text{S}$ ($\text{M}+\text{Na}$) $^+$ 432.0437, found 432.0417.

(E)-3-(2-chlorobenzylidene)-1-tosylindolin-2-one (**A4**): Yellow solid; yield: 40.4%; mp: 148.9–150.5 °C; ^1H NMR (600 MHz, DMSO- d_6): δ 7.98 (d, $J = 8.4$ Hz, 2H), 7.90 (d, $J = 8.3$ Hz, 1H), 7.73 (d, $J = 7.6$ Hz, 1H), 7.71 (s, 1H), 7.64 (d, $J = 8.0$ Hz, 1H), 7.55–7.52 (m, 1H), 7.50–7.46 (m, 4H), 7.21 (d, $J = 7.7$ Hz, 1H), 7.09 (t, $J = 7.7$ Hz, 1H), 2.39 (s, 3H); ^{13}C NMR (151 MHz, DMSO- d_6): δ 165.50, 146.62, 139.09, 135.69, 135.03, 133.31, 132.53, 132.42, 131.74, 130.74, 130.64, 130.43, 128.06, 127.93, 126.56, 125.22, 123.25, 121.13, 113.90, 21.65; HRMS calcd for $\text{C}_{22}\text{H}_{16}\text{ClNNaO}_3\text{S}$ ($\text{M}+\text{Na}$) $^+$ 432.0437, found 432.0416.

(E)-3-(2-chlorobenzylidene)-1-((2-chlorophenyl)sulfonyl)indolin-2-one (**A5**): Yellow solid; yield: 65.2%; mp: 157.2–158.1 °C; ^1H NMR (600 MHz, DMSO- d_6): δ 8.35 (dd, $J = 8.0, 1.4$ Hz, 1H), 7.82–7.79 (m, 2H), 7.76–7.70 (m, 4H), 7.65 (d, $J = 8.2$ Hz, 1H), 7.56–7.54 (m, 1H), 7.50–7.44 (m, 2H), 7.26 (d, $J = 7.8$ Hz, 1H), 7.11 (t, $J = 7.7$ Hz, 1H); ^{13}C NMR (151 MHz, DMSO- d_6): δ 165.4, 139.64, 136.92, 136.16, 135.37, 133.38, 133.29, 132.62, 132.52, 132.42, 131.80, 131.62, 130.65, 130.46, 128.65, 128.11, 126.13, 125.23, 123.30, 120.91, 114.44; HRMS calcd for $\text{C}_{21}\text{H}_{13}\text{Cl}_2\text{NNaO}_3\text{S}$ ($\text{M}+\text{Na}$) $^+$ 451.9891, found 451.9874.

(E)-3-(2-chlorobenzylidene)-1-((3-chlorophenyl)sulfonyl)indolin-2-one (**A6**): Yellow solid; yield: 45.2%; mp: 164.0–165.4 °C; ^1H NMR (600 MHz, DMSO- d_6): δ 8.11 (t, $J = 1.8$ Hz,

1H), 8.08 (d, $J = 8.0$ Hz, 1H), 7.91 (d, $J = 8.2$ Hz, 2H), 7.75–7.72 (m, 3H), 7.65 (d, $J = 8.0$ Hz, 1H), 7.56–7.53 (m, 1H), 7.50–7.46 (m, 2H), 7.23 (d, $J = 7.6$ Hz, 1H), 7.11 (t, $J = 7.4$ Hz, 1H); ^{13}C NMR (151 MHz, DMSO- d_6): δ 165.58, 138.84, 135.91, 135.67, 134.67, 133.34, 132.51, 132.48, 132.40, 131.75, 130.64, 130.45, 128.08, 127.52, 126.76, 126.48, 125.39, 123.28, 121.33, 113.94; HRMS calcd for $\text{C}_{21}\text{H}_{13}\text{Cl}_2\text{NNaO}_3\text{S}$ (M+Na) $^+$ 451.9891, found 451.9875.

(E)-3-(2-chlorobenzylidene)-1-((4-chlorophenyl)sulfonyl)indolin-2-one (**A7**): Yellow solid; yield: 43.6%; mp: 172.4–173.1 °C; ^1H NMR (600 MHz, DMSO- d_6): δ 8.11 (d, $J = 8.7$ Hz, 1H), 7.98 (d, $J = 8.6$ Hz, 1H), 7.89 (d, $J = 8.3$ Hz, 1H), 7.77 (d, $J = 8.7$ Hz, 2H), 7.71–7.70 (m, 2H), 7.65 (d, $J = 8.0$ Hz, 1H), 7.59 (d, $J = 8.4$ Hz, 1H), 7.56–7.53 (m, 1H), 7.36 (d, $J = 8.3$ Hz, 1H), 7.23 (d, $J = 7.7$ Hz, 1H), 7.10 (t, $J = 7.7$ Hz, 1H); ^{13}C NMR (151 MHz, DMSO- d_6): δ 165.56, 139.93, 139.57, 135.84, 133.33, 132.47, 131.75, 130.63, 130.49, 130.44, 129.95, 129.91, 128.15, 128.07, 127.94, 125.36, 123.29, 113.87; HRMS calcd for $\text{C}_{21}\text{H}_{14}\text{Cl}_2\text{NO}_3\text{S}$ (M+H) $^+$ 430.0071, found 430.1069.

(E)-3-(3-chlorobenzylidene)-1-(phenylsulfonyl)indolin-2-one (**A8**): Yellow solid; yield: 60.2%; mp: 115.1–117.3 °C; ^1H NMR (600 MHz, DMSO- d_6): δ 8.07 (d, $J = 7.7$ Hz, 2H), 8.04 (d, $J = 7.7$ Hz, 1H), 7.98 (s, 1H), 7.91 (d, $J = 8.2$ Hz, 1H), 7.86–7.84 (m, 1H), 7.79 (t, $J = 7.4$ Hz, 1H), 7.72 (s, 1H), 7.70–7.68 (m, 1H), 7.63–7.61 (m, 1H), 7.51 (d, $J = 7.7$ Hz, 2H), 7.44 (t, $J = 7.6$ Hz, 1H), 7.10 (t, $J = 7.7$ Hz, 1H); ^{13}C NMR (151 MHz, DMSO- d_6): δ 165.20, 138.37, 137.84, 137.35, 135.57, 135.01, 134.88, 133.43, 130.97, 130.59, 130.03, 129.91, 129.68, 129.65, 128.77, 127.44, 124.59, 122.39, 120.75, 113.30; HRMS calcd for $\text{C}_{21}\text{H}_{15}\text{ClNO}_3\text{S}$ (M+H) $^+$ 396.0461, found 396.0459.

(E)-3-(3-chlorobenzylidene)-1-(o-tolylsulfonyl)indolin-2-one (**A9**): Yellow solid; yield: 50.7%; mp: 140.9–143.2 °C; ^1H NMR (400 MHz, DMSO- d_6): δ 8.20–8.13 (m, 1H), 8.05 (s, 1H), 8.00–7.93 (m, 1H), 7.92–7.90 (m, 1H), 7.74–7.71 (m, 2H), 7.66 (d, $J = 7.5$ Hz, 1H), 7.56–7.51 (m, 3H), 7.49–7.44 (m, 2H), 7.16–7.10 (m, 1H); ^{13}C NMR (101 MHz, DMSO- d_6): δ 137.94, 135.62, 134.53, 133.44, 132.75, 130.89, 130.63, 130.06, 129.93, 128.79, 127.51, 127.27, 126.57, 124.45, 120.73, 120.59, 19.46; HRMS calcd for $\text{C}_{21}\text{H}_{16}\text{ClNNaO}_3\text{S}$ (M+Na) $^+$ 432.0437, found 432.0428.

(E)-3-(3-chlorobenzylidene)-1-(m-tolylsulfonyl)indolin-2-one (**A10**): Yellow solid; yield: 59.6%; mp: 147.4–149.2 °C; ^1H NMR (600 MHz, DMSO- d_6): δ 8.11 (d, 1H), 7.91–7.85 (m, 4H), 7.72 (m, 1H), 7.63–7.59 (m, 1H), 7.57–7.50 (m, 3H), 7.48–7.43 (m, 2H), 7.29–7.10 (m, 1H), 2.37 (d, 3H); ^{13}C NMR (151 MHz, DMSO- d_6): δ 165.76, 139.02, 138.41, 137.94, 136.27, 136.21, 136.15, 134.03, 131.57, 131.31, 131.21, 131.00, 130.65, 130.51, 130.11, 129.38, 128.05, 127.81, 127.63, 125.23, 125.16, 125.06, 125.02, 122.99, 113.55, 21.25; HRMS calcd for $\text{C}_{21}\text{H}_{16}\text{ClNNaO}_3\text{S}$ (M+Na) $^+$ 432.0437, found 432.0428.

(E)-3-(3-chlorobenzylidene)-1-tosylindolin-2-one (**A11**): Yellow solid; yield: 51.5%; mp: 136.3–138.1 °C; ^1H NMR (600 MHz, DMSO- d_6): δ 8.00 (d, $J = 5.5$ Hz, 1H), 7.96 (d, $J = 8.2$ Hz, 1H), 7.91 (t, $J = 8.3$ Hz, 1H), 7.86 (q, $J = 8.3$ Hz, 1H), 7.73 (d, $J = 5.0$ Hz, 1H), 7.65–7.55 (m, 2H), 7.53–7.49 (m, 3H), 7.48–7.44 (m, 2H), 7.30–7.12 (m, 1H); ^{13}C NMR (151 MHz, DMSO- d_6): δ 165.36, 146.13, 137.94, 130.87, 130.80, 130.27, 130.24, 130.08, 128.96, 127.63, 127.45, 127.38, 127.74, 124.13, 120.89, 113.48, 21.19; HRMS calcd for $\text{C}_{22}\text{H}_{17}\text{ClNO}_3\text{S}$ (M+H) $^+$ 410.0618, found 410.0612.

(E)-3-(3-chlorobenzylidene)-1-((2-chlorophenyl)sulfonyl)indolin-2-one (**A12**): Yellow solid; yield: 45.3%; mp: 125.1–126.3 °C; ^1H NMR (400 MHz, DMSO- d_6): δ 8.34 (t, $J = 6.7$, 1.2 Hz, 1H), 7.81 (t, $J = 8.1$ Hz, 2H), 7.72 (m, 4H), 7.55 (d, $J = 7.0$ Hz, 3H), 7.48–7.44 (m, 2H), 7.15 (t, $J = 7.7$ Hz, 1H); ^{13}C NMR (101 MHz, DMSO- d_6): δ 165.01, 139.04, 138.19, 137.54, 136.20, 135.50, 134.86, 133.45, 132.78, 131.95, 131.18, 130.81, 130.63, 130.34, 130.00, 128.82, 127.94, 127.49, 124.51, 122.42, 120.45, 113.83, 113.46; HRMS calcd for $\text{C}_{21}\text{H}_{14}\text{Cl}_2\text{NO}_3\text{S}$ (M+H) $^+$ 430.0071, found 430.0065.

(E)-3-(3-chlorobenzylidene)-1-((3-chlorophenyl)sulfonyl)indolin-2-one (**A13**): Yellow solid; yield: 48.8%; mp: 146.7–148.0 °C; ^1H NMR (400 MHz, DMSO- d_6): δ 8.21–8.12 (m, 2H), 8.06 (s, 1H), 7.95 (dd, $J = 7.0$ Hz, 1H), 7.82–7.74 (m, 2H), 7.71–7.65 (m, 1H), 7.53–7.47 (m, 4H), 7.33–7.25 (m, 1H), 7.15–7.11 (m, 1H); ^{13}C NMR (101 MHz, DMSO- d_6): δ 163.86, 139.36, 138.66, 137.59, 135.42, 133.36, 131.31, 131.24, 130.66, 128.08, 125.81, 125.78,

125.24, 124.61, 121.20, 114.08, 113.72; HRMS calcd for $C_{21}H_{13}Cl_2NNaO_3S$ (M+Na)⁺ 451.9891, found 451.9897.

(E)-3-(3-chlorobenzylidene)-1-((4-chlorophenyl)sulfonyl)indolin-2-one (**A14**): Yellow solid; yield: 39.2%; mp: 137.5–139.6 °C; ¹H NMR (400 MHz, DMSO-*d*₆): δ 8.32 (d, *J* = 7.9 Hz, 1H), 8.10 (d, *J* = 10.3 Hz, 2H), 7.94 (d, *J* = 7.7 Hz, 1H), 7.80–7.75 (m, 2H), 7.74–7.68 (m, 3H), 7.53 (d, *J* = 8.5 Hz, 2H), 7.44 (t, *J* = 7.6 Hz, 1H), 7.30 (t, *J* = 7.6 Hz, 1H); ¹³C NMR (101 MHz, DMSO-*d*₆): δ 139.53, 137.39, 136.09, 133.54, 132.69, 131.89, 131.06, 129.63, 128.38, 128.02, 124.50, 120.51, 113.41; HRMS calcd for $C_{22}H_{13}Cl_2NNaO_3S$ (M+Na)⁺ 451.9891, found 451.9884.

(E)-1-((2-bromophenyl) sulfonyl)-3-(3-chlorobenzylidene)indolin-2-one (**A15**): Yellow solid; yield: 41.6%; mp: 139.2–140.3 °C; ¹H NMR (400 MHz, DMSO-*d*₆): δ 8.37 (dd, *J* = 7.8, 1.7 Hz, 1H), 7.82 (d, *J* = 8.2 Hz, 1H), 7.73–7.69 (m, 3H), 7.69–7.65 (m, 2H), 7.57–7.54 (m, 3H), 7.48–7.44 (m, 2H), 7.14 (td, *J* = 7.7, 0.76 Hz, 1H); ¹³C NMR (101 MHz, DMSO-*d*₆): δ 164.96, 139.20, 138.11, 136.54, 136.00, 135.44, 135.40, 135.35, 133.41, 133.11, 130.75, 130.73, 130.58, 130.31, 130.00, 129.96, 128.79, 128.40, 128.33, 127.45, 124.56, 124.41, 122.36, 120.39, 119.58, 114.04; HRMS calcd for $C_{21}H_{13}ClBrNNaO_3S$ (M+Na)⁺ 495.9386, found 495.9383.

(E)-1-((3-bromophenyl) sulfonyl)-3-(3-chlorobenzylidene)indolin-2-one (**A16**): Yellow solid; yield: 47.4 %; mp: 111.3–112.9 °C; ¹H NMR (400 MHz, DMSO-*d*₆): δ 8.24–8.21 (m, 1H), 8.17–8.08 (m, 1H), 8.06–7.92 (m, 2H), 7.91–7.84 (m, 1H), 7.77–7.64 (m, 3H), 7.63–7.54 (m, 2H), 7.51–7.45 (q, 2H), 7.32–7.09 (m, 1H); ¹³C NMR (101 MHz, DMSO-*d*₆): δ 165.27, 139.03, 138.06, 137.92, 135.59, 131.00, 130.74, 130.66, 130.12, 130.07, 129.62, 128.82, 127.49, 126.43, 124.81, 124.75, 123.88, 122.43, 122.25, 120.92, 113.33, 112.94; HRMS calcd for $C_{21}H_{13}ClBrNNaO_3S$ (M+Na)⁺ 495.9386, found 495.9385.

(E)-1-((4-bromophenyl) sulfonyl)-3-(3-chlorobenzylidene)indolin-2-one (**A17**): Yellow solid; yield: 50.5%; mp: 131.7–132.5 °C; ¹H NMR (400 MHz, DMSO-*d*₆): δ 8.25–8.02 (m, 2H), 7.98 (d, *J* = 3.9 Hz, 1H), 7.97–7.92 (m, 1H), 7.92–7.83 (m, 3H), 7.73 (d, *J* = 7.8 Hz, 1H), 7.66–7.49 (m, 3H), 7.49–7.45 (m, 1H), 7.32–7.12 (td, *J* = 7.6 Hz, 1H); ¹³C NMR (101 MHz, DMSO-*d*₆): δ 165.20, 138.54, 137.92, 136.68, 136.51, 136.42, 135.55, 132.77, 130.69, 130.62, 130.40, 129.24, 128.76, 127.44, 124.99, 124.74, 124.68, 122.41, 120.85, 120.61, 113.25, 112.85; HRMS calcd for $C_{21}H_{13}ClBrNNaO_3S$ (M+Na)⁺ 495.9386, found 495.9388.

(E)-3-(3-chlorobenzylidene)-1-((2-fluorophenyl)sulfonyl)indolin-2-one (**A18**): Yellow solid; yield: 36.7%; mp: 158.2–160.3 °C; ¹H NMR (400 MHz, DMSO-*d*₆): δ 8.23–8.02 (m, 4H), 7.90–7.85 (m, 3H), 7.76–7.72 (m, 2H), 7.55–7.46 (m, 3H), 7.24–7.10 (m, 1H); ¹³C NMR (101 MHz, DMSO-*d*₆): δ 165.23, 138.96, 138.57, 137.98, 134.87, 134.04, 133.43, 131.74, 130.62, 130.05, 128.76, 127.44, 126.87, 126.06, 124.77, 124.71, 122.41, 120.90, 120.62, 113.32; HRMS calcd for $C_{21}H_{14}ClFNO_3S$ (M+H)⁺ 414.0367, found 414.0364.

(E)-3-(3-chlorobenzylidene)-1-((3-fluorophenyl)sulfonyl)indolin-2-one (**A19**): Yellow solid; yield: 35.0%; mp: 176.6–178.2 °C; ¹H NMR (400 MHz, DMSO-*d*₆): δ 8.23–7.98 (m, 2H), 7.94–7.82 (m, 2H), 7.74–7.62 (m, 4H), 7.53 (d, *J* = 5.5 Hz, 2H), 7.46 (t, *J* = 8.4 Hz, 2H), 7.12 (t, *J* = 7.3 Hz, 1H); ¹³C NMR (101 MHz, DMSO-*d*₆): δ 165.02, 138.41, 137.97, 137.78, 135.59, 133.25, 132.60, 131.99, 130.79, 130.54, 130.45, 129.87, 129.76, 128.58, 127.27, 124.82, 124.53, 123.40, 122.22, 120.69, 113.18, 112.78; HRMS calcd for $C_{21}H_{13}ClFNNaO_3S$ (M+Na)⁺ 436.0186, found 436.0184.

(E)-3-(3-chlorobenzylidene)-1-((4-fluorophenyl)sulfonyl)indolin-2-one (**A20**): Yellow solid; yield: 40.1%; mp: 141.7–143.1 °C; ¹H NMR (400 MHz, DMSO-*d*₆): δ 8.20–8.12 (m, 3H), 8.00 (d, *J* = 7.6 Hz, 1H), 7.93–7.84 (m, 2H), 7.73 (d, *J* = 9.1 Hz, 2H), 7.64 (d, *J* = 7.6 Hz, 1H), 7.55–7.48 (m, 3H), 7.12 (q, *J* = 7.6 Hz, 1H); ¹³C NMR (101 MHz, DMSO-*d*₆): δ 165.37, 138.65, 138.43, 138.01, 136.90, 135.72, 135.01, 133.72, 133.58, 132.93, 130.85, 128.93, 127.60, 124.84, 124.78, 122.55, 117.26, 117.03, 113.43, 106.96; HRMS calcd for $C_{21}H_{13}ClFNNaO_3S$ (M+Na)⁺ 436.0186, found 436.0185.

(E)-3-(3-chlorobenzylidene)-1-((3-(trifluoromethyl)phenyl)sulfonyl)indolin-2-one (**A21**): Yellow solid; yield: 38.9%; mp: 182.3–183.7 °C; ¹H NMR (400 MHz, DMSO-*d*₆): δ 8.18 (t, *J* = 3.6 Hz, 1H), 7.81 (s, 1H), 7.74–7.64 (m, 3H), 7.56–7.49 (m, 4H), 7.32 (d, *J* = 6.9 Hz, 1H), 7.26–7.20 (m, 1H), 7.00 (t, *J* = 7.6 Hz, 1H), 6.83 (d, *J* = 7.7 Hz, 1H); ¹³C NMR (101 MHz,

DMSO- d_6): δ 166.86, 140.93, 135.79, 135.49, 134.66, 133.37, 132.72, 130.67, 130.57, 130.52, 130.45, 129.87, 129.72, 129.35, 128.69, 128.03, 127.50, 124.41, 121.07, 119.99, 109.38; HRMS calcd for HRMS calcd for $C_{22}H_{14}ClF_3NO_3S$ (M+H)⁺ 464.0335, found 464.0331.

(E)-3-(3-chlorobenzylidene)-1-((3-nitrophenyl)sulfonyl)indolin-2-one (**A22**): Yellow solid; yield: 48.3%; mp: 195.3–197.0 °C; ¹H NMR (400 MHz, DMSO- d_6): δ 8.75–8.60 (m, 2H), 8.52 (d, J = 8.0 Hz, 1H), 8.03–7.87 (m, 3H), 7.78 (d, J = 8.7 Hz, 1H), 7.71 (d, J = 8.1 Hz, 1H), 7.55 (d, J = 6.5 Hz, 2H), 7.50 (d, J = 5.0 Hz, 2H), 7.16 (t, J = 7.6 Hz, 1H); ¹³C NMR (101 MHz, DMSO- d_6): δ 165.31, 147.82, 138.45, 138.12, 138.02, 135.55, 133.35, 131.68, 131.00, 130.66, 129.98, 129.45, 128.76, 127.44, 122.49, 122.45, 121.03, 113.23, 109.37; HRMS calcd for HRMS calcd for $C_{21}H_{13}ClN_2NaO_5S$ (M+Na)⁺ 463.0131, found 463.0131.

(E)-3-(3-chlorobenzylidene)-1-((4-methoxyphenyl)sulfonyl)indolin-2-one (**A23**): Yellow solid; yield: 46.6%; mp: 175.1–176.7 °C; ¹H NMR (400 MHz, DMSO- d_6): δ 8.05–8.00 (m, 2H), 7.91 (dd, J = 8.1, 3.1 Hz, 1H), 7.73–7.70 (m, 1H), 7.64 (d, J = 7.1 Hz, 1H), 7.55–7.49 (m, 2H), 7.47–7.43 (m, 2H), 7.20–7.14 (m, 3H), 7.09 (m, 1H); ¹³C NMR (101 MHz, DMSO- d_6): δ 164.21, 138.63, 137.67, 135.69, 135.01, 133.48, 131.17, 130.67, 130.09, 129.94, 129.89, 129.84, 129.75, 128.84, 127.51, 126.07, 124.58, 122.68, 120.54, 114.91, 114.86, 114.83, 113.33, 55.88; HRMS calcd for HRMS calcd for $C_{22}H_{17}ClNO_4S$ (M+H)⁺ 426.0567, found 426.0566.

(E)-3-(4-chlorobenzylidene)-1-(*o*-tolylsulfonyl)indolin-2-one (**A24**): Yellow solid; yield: 41.2%; mp: 155.2–157.1 °C; ¹H NMR (400 MHz, DMSO- d_6): δ 8.17–8.10 (m, 2H), 7.98–7.89 (m, 1H), 7.87–7.82 (m, 1H), 7.73–7.68 (m, 2H), 7.58–7.49 (m, 3H), 7.42 (t, J = 8.1 Hz, 3H), 7.15–7.09 (m, 1H), 2.43 (d, 3H); ¹³C NMR (101 MHz, DMSO- d_6): δ 165.18, 138.92, 138.34, 134.88, 134.58, 133.52, 132.71, 132.23, 131.12, 131.06, 130.69, 130.52, 130.03, 128.82, 128.30, 127.23, 126.52, 124.51, 124.41, 122.55, 122.39, 113.38, 113.23, 19.43; HRMS calcd for $C_{22}H_{16}ClNNaO_3SN_3O_2$ (M+Na)⁺ 432.0437, found 432.0431.

(E)-3-(4-chlorobenzylidene)-1-(*m*-tolylsulfonyl)indolin-2-one (**A25**): Yellow solid; yield: 50.9%; mp: 149.3–151.7 °C; ¹H NMR (400 MHz, DMSO- d_6): δ 8.15 (d, J = 8.6 Hz, 1H), 7.92–7.85 (m, 4H), 7.73 (t, J = 8.4 Hz, 2H), 7.59–7.55 (m, 4H), 7.48–7.43 (m, 1H), 7.30–7.11 (td, J = 7.6 Hz, 1H), 2.39 (d, 3H); ¹³C NMR (101 MHz, DMSO- d_6): δ 139.56, 138.96, 138.28, 135.66, 133.53, 132.30, 131.13, 130.84, 129.52, 128.88, 128.37, 127.20, 127.04, 124.60, 124.44, 123.11, 122.46, 113.29, 112.93, 20.66; HRMS calcd for $C_{22}H_{16}ClNNaO_3SN_3O_2$ (M+Na)⁺ 432.0437, found 432.0429.

(E)-3-(4-chlorobenzylidene)-1-tosylindolin-2-one (**A26**): Yellow solid; yield: 43.2%; mp: 134.1–135.6 °C; ¹H NMR (400 MHz, DMSO- d_6): δ 8.13 (d, J = 8.4 Hz, 1H), 7.99–7.85 (m, 4H), 7.70 (t, J = 5.8, 8.4 Hz, 2H), 7.56 (d, J = 8.4 Hz, 3H), 7.46 (d, J = 8.3 Hz, 2H), 7.20 (dd, J = 7.2 Hz, 1H), 2.36 (d, 3H); ¹³C NMR (101 MHz, DMSO- d_6): δ 138.75, 133.36, 130.95, 129.92, 128.70, 128.18, 127.10, 124.43, 20.87; HRMS calcd for $C_{22}H_{16}ClNNaO_3SN_3O_2$ (M+Na)⁺ 432.0437, found 432.0431.

(E)-3-(4-chlorobenzylidene)-1-((3-chlorophenyl)sulfonyl)indolin-2-one (**A27**): Yellow solid; yield: 44.9%; mp: 184.8–185.6 °C; ¹H NMR (400 MHz, DMSO- d_6): δ 8.09 (s, 1H), 8.08 (d, J = 8.1 Hz, 1H), 7.92–7.89 (m, 2H), 7.77 (s, 1H), 7.74–7.70 (m, 3H), 7.58 (d, J = 8.4 Hz, 3H), 7.46 (t, J = 8.0 Hz, 1H), 7.14 (t, J = 7.7 Hz, 1H); ¹³C NMR (101 MHz, DMSO- d_6): δ 138.51, 135.01, 131.77, 131.15, 130.85, 128.89, 126.88, 126.07, 124.78, 113.28; HRMS calcd for $C_{22}H_{13}Cl_2NNaO_3S$ (M+Na)⁺ 451.9891, found 451.9885.

(E)-3-(4-chlorobenzylidene)-1-(phenylsulfonyl)indolin-2-one (**A28**): Yellow solid; yield: 36.8%; mp: 135.4–136.8 °C; ¹H NMR (600 MHz, DMSO- d_6): δ 8.13 (d, J = 6.5 Hz, 1H), 8.08–7.99 (m, 2H), 7.91 (d, J = 7.1 Hz, 1H), 7.78–7.65 (m, 5H), 7.54 (m, 3H), 7.44 (d, J = 6.5 Hz, 1H), 7.11 (s, 1H); ¹³C NMR (151 MHz, DMSO- d_6): δ 165.94, 139.61, 138.90, 136.38, 135.60, 135.49, 134.13, 132.83, 131.71, 131.43, 130.40, 130.28, 130.23, 128.93, 127.78, 125.22, 124.95, 123.05, 121.06, 113.85, 113.48; HRMS calcd for $C_{21}H_{14}ClNNaO_3S$ (M+Na)⁺ 418.0281 found 418.0270.

(E)-5-chloro-3-(3-chlorobenzylidene)-1-((3-chlorophenyl)sulfonyl)indolin-2-one (**A29**): Yellow solid; yield: 39.3%; mp: 177.8–178.7 °C; ¹H NMR (400 MHz, DMSO- d_6): δ 8.11 (d, 1H), 8.05–8.02 (m, 2H), 7.91 (d, J = 8.7 Hz, 1H), 7.88–7.80 (m, 2H), 7.75 (s, 1H), 7.73–7.65 (m, 1H), 7.58–7.48 (m, 3H), 7.39–7.36 (m, 1H); ¹³C NMR (101 MHz, DMSO- d_6): δ 163.09, 140.38, 138.92, 135.33, 135.05, 134.73, 134.07, 132.92, 131.79, 131.76, 131.14, 130.98, 130.72,

130.26, 129.41, 129.34, 126.85, 126.24, 123.01, 120.59, 114.58; HRMS calcd for HRMS calcd for $C_{22}H_{12}Cl_3NNaO_3S$ (M+H)⁺ 485.9501, found 485.9499.

(E)-6-chloro-3-(3-chlorobenzylidene)-1-((3-chlorophenyl)sulfonyl)indolin-2-one (**A30**): Yellow solid; yield: 42.8%; mp: 132.6–133.8 °C; ¹H NMR (400 MHz, DMSO-*d*₆): δ 8.14–8.08 (m, 2H), 7.94–7.91 (m, 2H), 7.80 (s, 1H), 7.76–7.71 (m, 2H), 7.65 (d, *J* = 7.1 Hz, 1H), 7.58–7.53 (m, 2H), 7.49 (d, *J* = 8.4 Hz, 1H), 7.25 (dd, *J* = 8.4, 2.0 Hz, 1H); ¹³C NMR (101 MHz, DMSO-*d*₆): δ 139.39, 139.27, 136.01, 134.64, 134.11, 133.43, 132.31, 131.49, 131.34, 131.06, 130.78, 129.46, 128.08, 127.05, 125.27; HRMS calcd for HRMS calcd for $C_{22}H_{12}Cl_3NNaO_3S$ (M+H)⁺ 485.9501, found 485.9501.

3.4. General Procedure for Preparation of Target Compounds B1–B10

Based on the procedure for compounds **A1–A30**, target compounds **B1–B10** were obtained from intermediates **1–3** and the corresponding benzoyl chloride in the presence of NaOH in THF.

(E)-1-(2-chlorobenzoyl)-3-(2-chlorobenzylidene)indolin-2-one (**B1**): Yellow solid; yield: 27.9%; mp: 214.5–216.2 °C; ¹H NMR (400 MHz, DMSO-*d*₆): δ 7.78 (d, *J* = 7.2 Hz, 1H), 7.69 (s, 1H), 7.67–7.63 (m, 2H), 7.57–7.55 (m, 2H), 7.54–7.51 (m, 3H), 7.50–7.46 (m, 2H), 7.33 (d, *J* = 7.7 Hz, 1H), 7.17 (t, *J* = 7.6 Hz, 1H); ¹³C NMR (101 MHz, DMSO-*d*₆): δ 165.68, 139.39, 135.81, 134.45, 132.80, 132.46, 132.14, 131.77, 131.36, 130.87, 130.70, 130.50, 130.01, 129.88, 129.17, 129.02, 128.54, 127.51, 127.21, 127.10, 126.52, 125.23, 122.28, 121.42, 115.72; HRMS calcd for $C_{22}H_{13}Cl_2NNaO_2$ (M+Na)⁺ 416.0221, found 416.0213.

(E)-1-(3-chlorobenzoyl)-3-(2-chlorobenzylidene)indolin-2-one (**B2**): Yellow solid; yield: 37.3%; mp: 219.0–220.8 °C; ¹H NMR (400 MHz, DMSO-*d*₆): δ 8.26 (d, *J* = 8.1 Hz, 1H), 7.79–7.77 (m, 1H), 7.69–7.63 (m, 3H), 7.56–7.54 (m, 3H), 7.53–7.51 (m, 2H), 7.49–7.47 (m, 1H), 7.33 (d, *J* = 7.5 Hz, 1H), 7.17 (t, *J* = 7.6 Hz, 1H); ¹³C NMR (101 MHz, DMSO-*d*₆): δ 165.65, 139.36, 135.78, 134.41, 132.78, 132.11, 131.72, 131.32, 130.82, 130.68, 130.47, 129.97, 129.84, 128.99, 128.50, 127.46, 127.17, 127.06, 125.18, 122.24, 121.39, 115.69; HRMS calcd for $C_{22}H_{13}Cl_2NNaO_2$ (M+Na)⁺ 416.0221, found 416.0204.

(E)-1-(4-chlorobenzoyl)-3-(2-chlorobenzylidene)indolin-2-one (**B3**): Yellow solid; yield: 33.5%; mp: 221.3–222.7 °C; ¹H NMR (400 MHz, DMSO-*d*₆): δ 8.36 (dd, *J* = 7.8, 1.4 Hz, 1H), 7.83–7.79 (m, 2H), 7.77–7.70 (m, 4H), 7.65 (dd, *J* = 8.0, 1.1 Hz, 1H), 7.56–7.53 (m, 1H), 7.51–7.44 (m, 2H), 7.27 (d, *J* = 7.6 Hz, 1H), 7.11 (td, *J* = 7.7, 0.68 Hz, 1H); ¹³C NMR (101 MHz, DMSO-*d*₆): δ 164.78, 139.07, 136.27, 135.51, 134.81, 132.78, 132.71, 132.00, 131.88, 131.84, 131.21, 130.98, 130.05, 129.84, 128.02, 127.47, 125.53, 124.59, 122.69, 120.32, 113.84; HRMS calcd for $C_{22}H_{13}Cl_2NNaO_2$ (M+Na)⁺ 416.0221, found 416.0205.

(E)-3-(2-chlorobenzylidene)-1-(2-methylbenzoyl)indolin-2-one (**B4**): Yellow solid; yield: 36.7%; mp: 111.2–112.8 °C; ¹H NMR (600 MHz, DMSO-*d*₆): δ 8.09 (d, *J* = 7.7 Hz, 1H), 7.74 (d, *J* = 7.0 Hz, 1H), 7.62 (s, 1H), 7.52 (d, *J* = 7.0 Hz, 1H), 7.50–7.41 (m, 5H), 7.30 (d, *J* = 7.7 Hz, 2H), 7.29–7.26 (m, 1H), 7.13–6.98 (m, 1H), 2.29 (s, 3H); ¹³C NMR (151 MHz, DMSO-*d*₆): δ 166.40, 140.43, 136.20, 135.46, 134.55, 133.33, 132.75, 132.29, 131.29, 130.98, 130.81, 130.55, 130.43, 128.06, 127.87, 127.48, 126.02, 125.39, 122.76, 121.85, 116.07; HRMS calcd for $C_{23}H_{16}ClNNaO_2$ (M+Na)⁺ 396.0767, found 396.0750.

(E)-3-(2-chlorobenzylidene)-1-(3-methylbenzoyl)indolin-2-one (**B5**): Yellow solid; yield: 17.6%; mp: 128.2–129.7 °C; ¹H NMR (400 MHz, DMSO-*d*₆): δ 7.79–7.74 (m, 4H), 7.72 (s, 1H), 7.68–7.50 (m, 3H), 7.49–7.44 (m, 1H), 7.42 (t, *J* = 7.1 Hz, 3H), 7.36 (d, *J* = 7.5 Hz, 1H), 2.35 (s, 3H); ¹³C NMR (101 MHz, DMSO-*d*₆): δ 167.28, 137.75, 133.31, 130.57, 129.59, 128.30, 126.31; HRMS calcd for $C_{23}H_{16}ClNNaO_2$ (M+Na)⁺ 396.0767, found 396.0763.

(E)-3-(2-chlorobenzylidene)-1-(4-methylbenzoyl)indolin-2-one (**B6**): Yellow solid; yield: 20.7%; mp: 145.3–146.9 °C; ¹H NMR (400 MHz, DMSO-*d*₆): δ 7.80 (d, *J* = 6.6 Hz, 1H), 7.76–7.72 (m, 3H), 7.68 (s, 2H), 7.54 (t, *J* = 7.7, 6.6 Hz, 2H), 7.42 (t, *J* = 7.6 Hz, 1H), 7.34–7.29 (m, 3H), 7.10 (t, *J* = 7.6 Hz, 1H), 2.41 (s, 3H); ¹³C NMR (101 MHz, DMSO-*d*₆): δ 157.01, 133.73, 131.65, 130.52, 129.71, 128.65, 127.50, 124.26, 122.28, 114.65, 21.24; HRMS calcd for $C_{23}H_{16}ClNNaO_2$ (M+Na)⁺ 396.0767, found 396.0760.

(E)-1-(2-chlorobenzoyl)-3-(3-chlorobenzylidene)indolin-2-one (**B7**): Yellow solid; yield: 26.9%; mp: 108.3–109.7 °C; ^1H NMR (400 MHz, DMSO- d_6): δ 8.26 (d, J = 8.0 Hz, 1H), 7.75 (s, 1H), 7.72–7.68 (m, 2H), 7.64–7.60 (m, 2H), 7.58–7.54 (m, 3H), 7.51–7.46 (m, 3H), 7.22 (td, J = 7.7, 0.88 Hz, 1H); ^{13}C NMR (101 MHz, DMSO- d_6): δ 165.59, 139.27, 137.03, 135.79, 133.47, 131.33, 130.72, 130.68, 129.86, 129.13, 128.98, 128.78, 128.49, 127.43, 127.18, 125.66, 125.17, 122.02, 121.53, 115.65; HRMS calcd for $\text{C}_{22}\text{H}_{13}\text{Cl}_2\text{NNaO}_2$ (M+Na) $^+$ 416.0221, found 416.0224.

(E)-1-(3-chlorobenzoyl)-3-(3-chlorobenzylidene)indolin-2-one (**B8**): Yellow solid; yield: 19.9%; mp: 112.4–114.0 °C; ^1H NMR (400 MHz, DMSO- d_6): δ 7.92–7.87 (m, 3H), 7.75 (s, 2H), 7.71–7.68 (m, 3H), 7.57 (d, J = 3.6 Hz, 2H), 7.52 (d, J = 7.7 Hz, 1H), 7.44 (t, J = 7.6 Hz, 1H); ^{13}C NMR (101 MHz, DMSO- d_6): δ 166.04, 140.08, 136.49, 136.07, 133.55, 132.66, 132.01, 130.76, 130.60, 130.48, 129.99, 128.84, 128.79, 128.76, 127.87, 127.67, 127.52, 124.62, 122.04, 121.63, 115.16; HRMS calcd for $\text{C}_{22}\text{H}_{13}\text{Cl}_2\text{NNaO}_2$ (M+Na) $^+$ 416.0221, found 416.0222.

(E)-1-(4-chlorobenzoyl)-3-(3-chlorobenzylidene)indolin-2-one (**B9**): Yellow solid; yield: 22.5%; mp: 103.5–104.8 °C; ^1H NMR (400 MHz, DMSO- d_6): δ 7.93 (d, J = 8.2 Hz, 1H), 7.85 (t, J = 7.8, 8.1 Hz, 2H), 7.76 (s, 1H), 7.71 (s, 2H), 7.58 (d, J = 5.7 Hz, 5H), 7.45 (t, J = 7.7 Hz, 1H), 7.16 (t, J = 7.6 Hz, 1H); ^{13}C NMR (101 MHz, DMSO- d_6): δ 167.80, 140.24, 137.49, 136.60, 136.17, 133.63, 133.24, 131.36, 131.20, 130.88, 130.60, 129.93, 128.94, 128.81, 128.27, 127.62, 126.63, 124.65, 122.17, 121.64, 115.12; HRMS calcd for $\text{C}_{22}\text{H}_{13}\text{Cl}_2\text{NNaO}_2$ (M+Na) $^+$ 416.0221, found 416.0220.

(E)-1-(3-chlorobenzoyl)-3-(4-chlorobenzylidene)indolin-2-one (**B10**): Yellow solid; yield: 27.1%; mp: 141.3–142.3 °C; ^1H NMR (400 MHz, DMSO- d_6): δ 8.21 (dd, J = 8.1, 8.0 Hz, 1H), 8.07 (t, J = 8.6, 6.2 Hz, 1H), 7.97–7.75 (m, 1H), 7.73–7.68 (m, 2H), 7.63–7.59 (m, 2H), 7.56–7.51 (m, 3H), 7.49–7.44 (m, 2H), 7.38–7.20 (m, 1H); ^{13}C NMR (101 MHz, DMSO- d_6): δ 166.20, 138.06, 136.43, 135.35, 133.99, 133.02, 131.67, 131.14, 129.48, 129.07, 128.92, 127.77, 125.76, 125.71, 125.56, 122.65, 122.19, 116.16; HRMS calcd for $\text{C}_{22}\text{H}_{13}\text{Cl}_2\text{NNaO}_2$ (M+Na) $^+$ 416.0221, found 416.0223.

3.5. In Vitro Enzymatic Assays

Dose-dependent MDM2 and MDMX binding evaluations were carried out using the fluorescence polarization assay.

A total of 30 nM preincubated (30 min) MDM2 (or MDMX) and 10 nM PMDM-F peptide in reaction buffer (100 μL , potassium phosphate, 100 mM; bovine gamma globulin, 100 mg/mL; sodium azide, 0.02%) were added into a 96-well plate containing the tested compounds at pH 7.5. The plate was incubated at 37 °C for 30 min and the polarization values were measured (485 nm excitation, 528 nm static, and polarized filter). The K_i values were calculated according to a reported method [41].

3.6. MTT Assay in Vitro

All compounds with K_i values of <1 μM toward MDM2 in the fluorescence polarization assay were evaluated against the MCF7, HCT116, and A549 cell lines (ATCC, Manassas, VA, USA) in vitro using a standard MTT assay, with nutlin-3a as a positive control. Compounds were tested at six concentrations (0.001–100 μM).

The cells were seeded into a 96-well plate and allowed to attach overnight, after which various concentrations of test compounds or DMSO were added to the culture medium and the cells were incubated for 48 h at 37 °C in a 5% CO_2 humidified incubator. Then, 20 μL of 0.5% the fresh MTT solution was added to each well. After incubation for another 4 h, the culture medium was removed and 150 μL of DMSO was added to dissolve the formazan crystals. The absorbance at 540 nm was measured using a microplate reader. The results, expressed as IC_{50} values, were the average of three determinations and were calculated using nonlinear regression analysis.

3.7. Western Blotting Assay

The HCT116 cells with wild type p53 were treated with compound **A13** (0, 5, 10, and 20 μM) for 48 h. The cells were harvested and lysed with RIPA buffer (Sigma, St. Louis, MI, USA) supplemented with a protease inhibitor cocktail (Sigma), followed by centrifugation at $12,000\times g$ for 10 min. The supernatants were heated to $100\text{ }^{\circ}\text{C}$ with loading buffer and the total protein concentrations were determined using a Bio-Rad protein assay. Protein samples were subjected to SDS-PAGE and transferred to a PVDF membrane. The membrane was blocked with 5% non-fat milk, and then incubated with the corresponding primary antibody (MDM2, MDMX, p53, and GAPDH) at $4\text{ }^{\circ}\text{C}$ overnight. After binding with an appropriate secondary antibody conjugated with peroxidase, proteins were visualized using the ECL chemiluminescence system. GAPDH was used as a loading control.

3.8. Molecular Docking

Molecular docking analysis was carried out using Sybyl-X2.0. The crystal structures of MDM2 (PDB code: 3LBL) and MDMX (PDB code: 2N0W) were processed. The ligand and the water molecules were first removed and the hydrogen atoms were added. The biopolymer was protonated at pH 7.4 and the Amber7 FF99 force field was applied. Other parameters were set at the default. The minimized protein and compound **A13** were subjected to the docking protocol using the Surflex-Dock Geom mode of Sybyl-X2.0.

4. Conclusions

In this study, a library of new indolone derivatives was synthesized and evaluated for their biological activity. The preliminary structure–activity relationship study showed that the compounds with benzene sulfonyl groups demonstrated a higher potency than the benzene sulfonamide groups. The 3-substituted electron-withdrawing group at the R_3 position is necessary ($3\text{-Cl} > 3\text{-F} > 3\text{-Br} > 3\text{-CF}_3 > 3\text{-NO}_2$) to increase the affinity to the enzyme. All of the compounds exhibited better activities to MDM2 than MDMX. Compound **A13** was identified as having the most potent affinity toward MDM2 and MDMX through the fluorescence polarization assay, with a K_i of 0.031 and 7.24 μM , respectively. The docking studies demonstrated that compound **A13** formed hydrophobic interactions with Leu54, Tyr67, His73, Val93, His96, Ile99, and Tyr100 in the MDM2 active site, and Met53, Ile60, Met61, Tyr66, and Val92 in the MDMX active site. **A13** also exhibited a greater potency than nutlin-3a against the HCT116, MCF7, and 143B cell lines. The Western blot analysis showed that **A13** induced accumulations of MDM2, MDMX, and p53, suggesting the activation of the p53 pathway.

Supplementary Materials: The following supporting information can be downloaded at: <https://www.mdpi.com/article/10.3390/molecules27123721/s1>, the ^1H NMR spectrum, ^{13}C NMR spectrum, and mass spectrum of compounds **1–5**, **A1–A30**, and **B1–B10**.

Author Contributions: Y.W. carried out the experiments and wrote the paper; B.J. and Z.C. synthesized the compounds; L.Z., Y.C., and Y.L. evaluated the biological activities of the target compounds; J.R. contributed to the data analysis of the biological tests; W.L. contributed to the data analysis of the NMR spectrum; Y.M. contributed to the analysis of molecular docking. All authors have read and agreed to the published version of the manuscript.

Funding: The work was supported by the National Natural Science Foundation of China (21867013, 81860631, 21967013) and the Jiangxi Provincial Natural Science Foundation (20202BABL216077, 20192BAB215043).

Institutional Review Board statement: Not applicable.

Informed Consent Statement: Not applicable.

Data Availability Statement: The data presented in this study are available on request from the corresponding author.

Conflicts of Interest: The authors declare no conflict of interest.

Sample Availability: Samples of the compounds are available from the authors.

References

1. Zhuang, C.; Miao, Z.; Zhu, L.; Dong, G.; Guo, Z.; Wang, S.; Zhang, Y.; Wu, Y.; Yao, J.; Sheng, C.; et al. Discovery, synthesis, and biological evaluation of orally active pyrrolidone derivatives as novel inhibitors of p53-MDM2 protein-protein interaction. *J. Med. Chem.* **2012**, *55*, 9630–9642. [CrossRef] [PubMed]
2. Ding, K.; Lu, Y.; Nikolovska-Coleska, Z.; Wang, G.; Qiu, S.; Shangary, S.; Gao, W.; Qin, D.; Stuckey, J.; Krajewski, K.; et al. Structure-based design of spiro-oxindoles as potent, specific small-molecule inhibitors of the MDM2-p53 interaction. *J. Med. Chem.* **2006**, *49*, 3432–3435. [CrossRef] [PubMed]
3. Twarda-Clapa, A.; Krzanik, S.; Kubica, K.; Guzik, K.; Labuzek, B.; Neochoritis, C.G.; Khoury, K.; Kowalska, K.; Czub, M.; Dubin, G.; et al. 1,4,5-Trisubstituted Imidazole-Based p53-MDM2/MDMX Antagonists with Aliphatic Linkers for Conjugation with Biological Carriers. *J. Med. Chem.* **2017**, *60*, 4234–4244. [CrossRef]
4. Rew, Y.; Sun, D. Discovery of a small molecule MDM2 inhibitor (AMG 232) for treating cancer. *J. Med. Chem.* **2014**, *57*, 6332–6341. [CrossRef] [PubMed]
5. Fry, D.C.; Emerson, S.D.; Palme, S.; Vu, B.T.; Liu, C.M.; Podlaski, F. NMR structure of a complex between MDM2 and a small molecule inhibitor. *J. Biomol. NMR* **2004**, *30*, 163–173. [CrossRef] [PubMed]
6. Ding, K.; Lu, Y.; Nikolovska-Coleska, Z.; Qiu, S.; Ding, Y.; Gao, W.; Stuckey, J.; Krajewski, K.; Roller, P.P.; Tomita, Y.; et al. Structure-based design of potent non-peptide MDM2 inhibitors. *J. Am. Chem. Soc.* **2005**, *127*, 10130–10131. [CrossRef]
7. Koblisch, H.K.; Zhao, S.; Franks, C.F.; Donatelli, R.R.; Tominovich, R.M.; LaFrance, L.V.; Leonard, K.A.; Gushue, J.M.; Parks, D.J.; Calvo, R.R.; et al. Benzodiazepinedione inhibitors of the Hdm2:p53 complex suppress human tumor cell proliferation in vitro and sensitize tumors to doxorubicin in vivo. *Mol. Cancer Ther.* **2006**, *5*, 160–169. [CrossRef]
8. Rothweiler, U.; Czarna, A.; Krajewski, M.; Ciombor, J.; Kalinski, C.; Khazak, V.; Ross, G.; Skobeleva, N.; Weber, L.; Holak, T.A. Isoquinolin-1-one inhibitors of the MDM2-p53 interaction. *Chem. Med. Chem.* **2008**, *3*, 1118–1128. [CrossRef]
9. Allen, J.G.; Bourbeau, M.P.; Wohlhieter, G.E.; Bartberger, M.D.; Michelsen, K.; Hungate, R.; Gadwood, R.C.; Gaston, R.D.; Evans, B.; Mann, L.W.; et al. Discovery and optimization of chromenotriazolopyrimidines as potent inhibitors of the mouse double minute 2-tumor protein 53 protein-protein interaction. *J. Med. Chem.* **2009**, *52*, 7044–7053. [CrossRef]
10. Furet, P.; Chene, P.; De Pover, A.; Valat, T.S.; Lisztwan, J.H.; Kallen, J.; Masuya, K. The central valine concept provides an entry in a new class of non peptide inhibitors of the p53-MDM2 interaction. *Bioorg. Med. Chem. Lett.* **2012**, *22*, 3498–3502. [CrossRef]
11. Yang, M.C.; Peng, C.; Huang, H.; Yang, L.; He, X.H.; Huang, W.; Cui, H.L.; He, G.; Han, B. Organocatalytic Asymmetric Synthesis of Spiro-oxindole Piperidine Derivatives That Reduce Cancer Cell Proliferation by Inhibiting MDM2-p53 Interaction. *Org. Lett.* **2017**, *19*, 6752–6755. [CrossRef] [PubMed]
12. Kumar, S.K.; Hager, E.; Pettit, C.; Gurulingappa, H.; Davidson, N.E.; Khan, S.R. Design, Synthesis, and Evaluation of Novel Boronic-Chalcone Derivatives as Antitumor Agents. *J. Med. Chem.* **2003**, *46*, 2813–2815. [CrossRef] [PubMed]
13. Pettersson, M.; Quant, M.; Min, J.; Iconaru, L.; Kriwacki, R.W.; Waddell, M.B.; Guy, R.K.; Luthman, K.; Grotli, M. Design, Synthesis and Evaluation of 2,5-Diketopiperazines as Inhibitors of the MDM2-p53 Interaction. *PLoS ONE* **2015**, *10*, e0137867. [CrossRef] [PubMed]
14. Gonzalez, A.Z.; Eksterowicz, J.; Bartberger, M.D.; Beck, H.P.; Canon, J.; Chen, A.; Chow, D.; Duquette, J.; Fox, B.M.; Fu, J.; et al. Selective and potent morpholinone inhibitors of the MDM2-p53 protein-protein interaction. *J. Med. Chem.* **2014**, *57*, 2472–2488. [CrossRef]
15. Surmiak, E.; Twarda-Clapa, A.; Zak, K.M.; Musielak, B.; Tomala, M.D.; Kubica, K.; Grudnik, P.; Madej, M.; Jablonski, M.; Potempa, J.; et al. A Unique Mdm2-Binding Mode of the 3-Pyrrolin-2-one- and 2-Furanone-Based Antagonists of the p53-Mdm2 Interaction. *ACS Chem. Biol.* **2016**, *11*, 3310–3318. [CrossRef]
16. Andreeff, M.; Kelly, K.R.; Yee, K.; Assouline, S.; Strair, R.; Popplewell, L.; Bowen, D.; Martinelli, G.; Drummond, M.W.; Vyas, P.; et al. Results of the Phase I Trial of RG7112, a Small-Molecule MDM2 Antagonist in Leukemia. *Clin. Cancer Res.* **2016**, *22*, 868–876. [CrossRef]
17. Zanjirband, M.; Edmondson, R.J.; Lunec, J. Pre-clinical efficacy and synergistic potential of the MDM2-p53 antagonists, Nutlin-3 and RG7388, as single agents and in combined treatment with cisplatin in ovarian cancer. *Oncotarget* **2016**, *7*, 40115–40134. [CrossRef] [PubMed]
18. De Jonge, M.; de Weger, V.A.; Dickson, M.A.; Langenberg, M.; Le Cesne, A.; Wagner, A.J.; Hsu, K.; Zheng, W.; Mace, S.; Tuffal, G.; et al. A phase I study of SAR405838, a novel human double minute 2 (HDM2) antagonist, in patients with solid tumours. *Eur. J. Cancer* **2017**, *76*, 144–151. [CrossRef]
19. Sun, D.; Li, Z.; Rew, Y.; Gribble, M.; Bartberger, M.D.; Beck, H.P.; Canon, J.; Chen, A.; Chen, X.; Chow, D.; et al. Discovery of AMG 232, a potent, selective, and orally bioavailable MDM2-p53 inhibitor in clinical development. *J. Med. Chem.* **2014**, *57*, 1454–1472. [CrossRef]
20. Novartis Pharmaceuticals. Study of Safety and Efficacy of HDM201 in Combination With LEE011 in Patients With Liposarcoma. ClinicalTrials. Gov Identifier: NCT02343172. 2015. Available online: <https://clinicaltrials.gov/ct2/show/NCT02343172> (accessed on 15 May 2022).

21. Aguilar, A.; Lu, J.; Liu, L.; Du, D.; Bernard, D.; McEachern, D.; Przybranowski, S.; Li, X.; Luo, R.; Wen, B.; et al. Discovery of 4-((3'R,4'S,5'R)-6''-Chloro-4'-(3-chloro-2-fluorophenyl)-1'-ethyl-2''-oxodispiro[cyclohexane-1,2'pyrrolidine-3',3''-indoline]-5'-carboxamido)bicyclo[2.2.2]octane-1-carboxylic Acid (AA-115/APG-115): A Potent and Orally Active Murine Double Minute 2 (MDM2) Inhibitor in Clinical Development. *J. Med. Chem.* **2017**, *60*, 2819–2839.
22. Reed, D.; Shen, Y.; Shelat, A.A.; Arnold, L.A.; Ferreira, A.M.; Zhu, F.; Mills, N.; Smithson, D.C.; Regni, C.A.; Bashford, D.; et al. Identification and characterization of the first small molecule inhibitor of MDMX. *J. Biol. Chem.* **2010**, *285*, 10786–10796. [[CrossRef](#)] [[PubMed](#)]
23. Wang, H.; Ma, X.; Ren, S.; Buolamwini, J.K.; Yan, C. A small-molecule inhibitor of MDMX activates p53 and induces apoptosis. *Mol. Cancer Ther.* **2011**, *10*, 69–79. [[CrossRef](#)] [[PubMed](#)]
24. Zhang, J.; Yu, G.; Yang, Y.; Wang, Y.; Guo, M.; Yin, Q.; Yan, C.; Tian, J.; Fu, F.; Wang, H. A small-molecule inhibitor of MDMX suppresses cervical cancer cells via the inhibition of E6-E6AP-p53 axis. *Pharmacol. Res.* **2022**, *177*, 106128. [[CrossRef](#)] [[PubMed](#)]
25. Qin, L.; Yang, F.; Zhou, C.; Chen, Y.; Zhang, H.; Su, Z. Efficient reactivation of p53 in cancer cells by a dual MdmX/Mdm2 inhibitor. *J. Am. Chem. Soc.* **2014**, *136*, 18023–18033. [[CrossRef](#)]
26. Golestanian, S.; Sharifi, A.; Popowicz, G.M.; Azizian, H.; Foroumadi, A.; Szwagierczak, A.; Holak, T.A.; Amanlou, M. Discovery of novel dual inhibitors against Mdm2 and Mdmx proteins by in silico approaches and binding assay. *Life Sci.* **2016**, *145*, 240–246. [[CrossRef](#)]
27. Lee, X.A.; Verma, C.; Sim, A.Y.L. Designing dual inhibitors of Mdm2/MdmX: Unexpected coupling of water with gatekeeper Y100. *Proteins* **2017**, *85*, 1493–1506. [[CrossRef](#)]
28. Mrkvova, Z.; Uldrijan, S.; Pombinho, A.; Bartunek, P.; Slaninova, I. Benzimidazoles Downregulate Mdm2 and MdmX and Activate p53 in MdmX Overexpressing Tumor Cells. *Molecules* **2019**, *24*, 2152. [[CrossRef](#)]
29. Muhammad, I.; Rahman, N.; Nayab, G.E.; Niaz, S.; Shah, M.; Afridi, S.G.; Khan, H.; Daglia, M.; Capanoglu, E. The Molecular Docking of Flavonoids Isolated from *Daucus carota* as a Dual Inhibitor of MDM2 and MDMX. *Recent Pat. Anticancer Drug Discov.* **2020**, *15*, 154–164. [[CrossRef](#)]
30. Pairawan, S.; Zhao, M.; Yuca, E.; Annis, A.; Evans, K.; Sutton, D.; Carvajal, L.; Ren, J.G.; Santiago, S.; Guerlavais, V.; et al. First in class dual MDM2/MDMX inhibitor ALRN-6924 enhances antitumor efficacy of chemotherapy in TP53 wild-type hormone receptor-positive breast cancer models. *Breast Cancer Res.* **2021**, *23*, 29. [[CrossRef](#)]
31. Saleh, M.N.; Patel, M.R.; Bauer, T.M.; Goel, S.; Falchook, G.S.; Shapiro, G.I.; Chung, K.Y.; Infante, J.R.; Conry, R.M.; Rabinowits, G.; et al. Phase 1 Trial of ALRN-6924, a Dual Inhibitor of MDMX and MDM2, in Patients with Solid Tumors and Lymphomas Bearing Wild-type TP. *Clin. Cancer Res.* **2021**, *27*, 5236–5247. [[CrossRef](#)]
32. Wan, Y.; Li, Y.; Yan, C.; Yan, M.; Tang, Z. Indole: A privileged scaffold for the design of anti-cancer agents. *Eur. J. Med. Chem.* **2019**, *183*, 111691. [[CrossRef](#)] [[PubMed](#)]
33. Cilibrasi, V.; Spano, V.; Bortolozzi, R.; Barreca, M.; Raimondi, M.V.; Rocca, R.; Maruca, A.; Montalbano, A.; Alcaro, S.; Ronca, R.; et al. Synthesis of 2H-Imidazo[2',1':2,3] [1,3]thiazolo[4,5-e]isoindol-8-yl-phenylureas with promising therapeutic features for the treatment of acute myeloid leukemia (AML) with FLT3/ITD mutations. *Eur. J. Med. Chem.* **2022**, *235*, 114292. [[CrossRef](#)] [[PubMed](#)]
34. Yu, Z.; Chen, Z.; Su, Q.; Ye, S.; Yuan, H.; Kuai, M.; Lv, M.; Tu, Z.; Yang, X.; Liu, R.; et al. Dual inhibitors of RAF-MEK-ERK and PI3K-PDK1-AKT pathways: Design, synthesis and preliminary anticancer activity studies of 3-substituted-5-(phenylamino) indolone derivatives. *Bioorg. Med. Chem.* **2019**, *27*, 944–954. [[CrossRef](#)] [[PubMed](#)]
35. Spano, V.; Barreca, M.; Rocca, R.; Bortolozzi, R.; Bai, R.; Carbone, A.; Raimondi, M.V.; Piccionello, A.P.; Montalbano, A.; Alcaro, S.; et al. Insight on [1,3]thiazolo[4,5-e]isoindoles as tubulin polymerization inhibitors. *Eur. J. Med. Chem.* **2021**, *212*, 113122. [[CrossRef](#)] [[PubMed](#)]
36. Zheng, G.H.; Shen, J.J.; Zhan, Y.C.; Yi, H.; Xue, S.T.; Wang, Z.; Ji, X.Y.; Li, Z.R. Design, synthesis and in vitro and in vivo antitumour activity of 3-benzylideneindolin-2-one derivatives, a novel class of small-molecule inhibitors of the MDM2-p53 interaction. *Eur. J. Med. Chem.* **2014**, *81*, 277–288. [[CrossRef](#)] [[PubMed](#)]
37. Barreca, M.; Spanò, V.; Raimondi, M.V.; Montalbano, A.; Bai, R.; Gaudio, E.; Alcaro, S.; Hamel, E.; Bertoni, F.; Barraja, P. Evaluation of [1,2]oxazolo[5,4-e]isoindoles in lymphoma cells. *Eur. J. Cancer* **2020**, *138*, 35–36. [[CrossRef](#)]
38. Barreca, M.; Ingarra, A.M.; Raimondi, M.V.; Spano, V.; De Franco, M.; Menilli, L.; Gandin, V.; Miolo, G.; Barraja, P.; Montalbano, A. Insight on pyrimido[5,4-g]indolizine and pyrimido[4,5-c]pyrrolo[1,2-a]azepine systems as promising photosensitizers on malignant cells. *Eur. J. Med. Chem.* **2022**, *237*, 114399. [[CrossRef](#)]
39. Zhang, S.; Lou, J.; Li, Y.; Zhou, F.; Yan, Z.; Lyu, X.; Zhao, Y. Recent Progress and Clinical Development of Inhibitors that Block MDM4/p53 Protein-Protein Interactions. *J. Med. Chem.* **2021**, *64*, 10621–10640. [[CrossRef](#)]
40. Popowicz, G.M.; Czarna, A.; Wolf, S.; Wang, K.; Wang, W.; Domling, A.; Holak, T.A. Structures of low molecular weight inhibitors bound to MDMX and MDM2 reveal new approaches for p53-MDMX/MDM2 antagonist drug discovery. *Cell Cycle* **2010**, *9*, 1104–1111. [[CrossRef](#)]
41. Nikolovska-Coleska, Z.; Wang, R.; Fang, X.; Pan, H.; Tomita, Y.; Li, P.; Roller, P.P.; Krajewski, K.; Saito, N.G.; Stuckey, J.A.; et al. Development and optimization of a binding assay for the XIAP BIR3 domain using fluorescence polarization. *Anal. Biochem.* **2004**, *332*, 261–273. [[CrossRef](#)]